

1 **ASSESSMENT OF PAVEMENT DEFLECTION-CAUSED FUEL**  
2 **CONSUMPTION VIA FWD DATA**  
3  
4

5 Abbas Booshehrian, Ph.D. Candidate – Corresponding Author  
6 Department of Civil, Environmental, and Geo- Engineering  
7 University of Minnesota  
8 179 Civil Engineering Building, 500 Pillsbury Drive S.E.,  
9 Minneapolis, MN 55455-0116  
10 Phone: (508) 971-3735  
11 Fax: (612) 626-7750  
12 Email: [boosh002@umn.edu](mailto:boosh002@umn.edu)  
13

14 Arghavan Louhghalam, Ph.D.  
15 Department of Civil & Environmental Engineering  
16 Massachusetts Institute of Technology  
17 77 Massachusetts Ave, Room 1-382,  
18 Cambridge, MA 02139  
19 Email: [arghavan@mit.edu](mailto:arghavan@mit.edu)  
20

21 Lev Khazanovich, Ph.D.  
22 Department of Civil, Environmental, and Geo- Engineering  
23 University of Minnesota  
24 160 Civil Engineering Building, 500 Pillsbury Drive S.E.,  
25 Minneapolis, MN 55455-0116  
26 Phone: (612) 624-4764  
27 Fax: (612) 626-7750  
28 Email: [khaza001@umn.edu](mailto:khaza001@umn.edu)  
29

30 Franz-Josef Ulm, Ph.D.  
31 Department of Civil & Environmental Engineering  
32 Massachusetts Institute of Technology  
33 Bldg. 1-263, 77 Massachusetts Avenue  
34 Cambridge, MA 02139  
35 Phone: 617-253.3544  
36 Email: [ulm@mit.edu](mailto:ulm@mit.edu)  
37  
38  
39

40 Submission Date: August 1<sup>st</sup>, 2015  
41

42 Word Count = 5,352  
43 Tables x 250 Words = 3 x 250 = 750  
44 Figures x 250 Words = 4 x 250 = 1,000  
45

46 Total Equivalent Word Count = 7,106  
47

**1 ABSTRACT**

2 The recently developed deflection-induced pavement-vehicle interaction analysis links the  
3 structural performance of the pavement to the fuel consumption of moving vehicles and the  
4 subsequent greenhouse gas emissions during the pavement use-phase. Accurate estimations of  
5 these impacts are tightly dependent on the proper evaluation of pavement structural parameters,  
6 including the properties of the surface course and underlying layers. A recent study demonstrated  
7 that inertia and damping effects of underlying layers must be taken into account for pavements  
8 subjected to dynamic loads, and that accurate parameters of pavement model could be  
9 backcalculated using the falling weight deflectometer measurements. In this paper, the  
10 pavement-vehicle interaction analysis is modified accordingly. Then, a case study is performed  
11 using multiple time histories of falling weight deflectometer deflections collected over a year's  
12 time for a rigid and a flexible pavement. Analysis of deflection basins showcases how falling  
13 weight deflectometer measurements can be used for estimating the deflection-induced vehicle  
14 fuel consumption for both rigid and flexible pavements. The simplicity and accuracy of the  
15 demonstrated analyses show a lot of promise for wider application of this methodology,  
16 especially regarding sustainable development of pavement network.

17

## 1 BACKGROUND

2 It is well established that road properties affect rolling resistance, and thus, fuel consumption and  
3 corresponding environmental footprint (1-4). Alongside pavement roughness and texture (5-8),  
4 dissipation of energy due to pavement deformation is an important contributor to rolling  
5 resistance (9). The deflection-induced dissipated energy contributes to excess fuel consumption  
6 and use-phase greenhouse gas emission. In order to develop sustainable transportation systems, it  
7 is necessary to develop quantitative tools that establish the link between pavement deformation  
8 and life-cycle energy consumption, which has been the topic of few recent studies (6,9-11).  
9 Some quantitative tools have been proposed. For instance, deflections recorded by Benkelman  
10 beam rebound were used by Zaabar and Chatti as an indicating factor in estimating the fuel  
11 consumption (6). Another approach was the deflection-induced pavement-vehicle interaction  
12 (PVI) model proposed by Louhghalam et al. PVI quantifies the dissipated energy due to viscous  
13 deformation of pavement under a moving load and evaluates the related fuel consumption and  
14 environmental footprint as functions of structural and material properties of pavement (12,13).

15  
16 In order to determine the surface deformation and the resulting dissipated energy, the PVI  
17 model proposed by Louhghalam et al. (12) idealizes both rigid and flexible pavements as a  
18 viscoelastic plate resting on a weightless elastic Winkler foundation. This model is  
19 computationally efficient, and so it is an attractive tool for an analysis that up-scales the  
20 pavement-scale emission to network level environmental impact (14,15). However, the  
21 simplicity of this model does not guarantee its ability to properly describe the pavement  
22 behavior. Especially for the case of a flexible pavement, the use of a Winkler foundation model  
23 is not a common practice. Therefore, the accuracy of this idealization must be tested when  
24 pavement is subjected to dynamic loads. Also, regardless of the accuracy of the selected model,  
25 pavement structural parameters are needed to perform the PVI analysis.

26  
27 The dynamic nature of the falling weight deflectometer (FWD) loading mechanism and  
28 its similarity with moving loads make the FWD time history deflection data a viable source for  
29 1) evaluation of the ability of the selected model in describing the pavement behavior, and 2)  
30 development of a rational approach for the assignment of model parameters for PVI analysis.  
31 Since FWDs are commonly used by roadway agencies, the FWD deflection data could be used  
32 for rational analysis of vehicles fuel consumption on roadways in network planning and  
33 pavement management decision-making.

34  
35 A numerical-based dynamic backcalculation method was recently developed to analyze  
36 the FWD deflection time histories and indicate the pavement model parameters (16). As the  
37 forward model of this backcalculation method, the generalized Westergaard model was used  
38 which accounts for the inertia and damping effects of foundation as well as the viscoelasticity of  
39 the plate (16). By performing a field study on two FWD deflection basins obtained from adjacent  
40 rigid and flexible pavements in Minnesota, it was shown that including both inertia and damping  
41 effects of foundation is substantial for accurate description of the behavior of both rigid and  
42 flexible pavements under dynamic loading. Therefore, in order to obtain realistic estimations for  
43 the dissipated energy, the deflection-induced PVI model proposed by Louhghalam et al. needs to  
44 be modified to account for foundation inertia and damping.

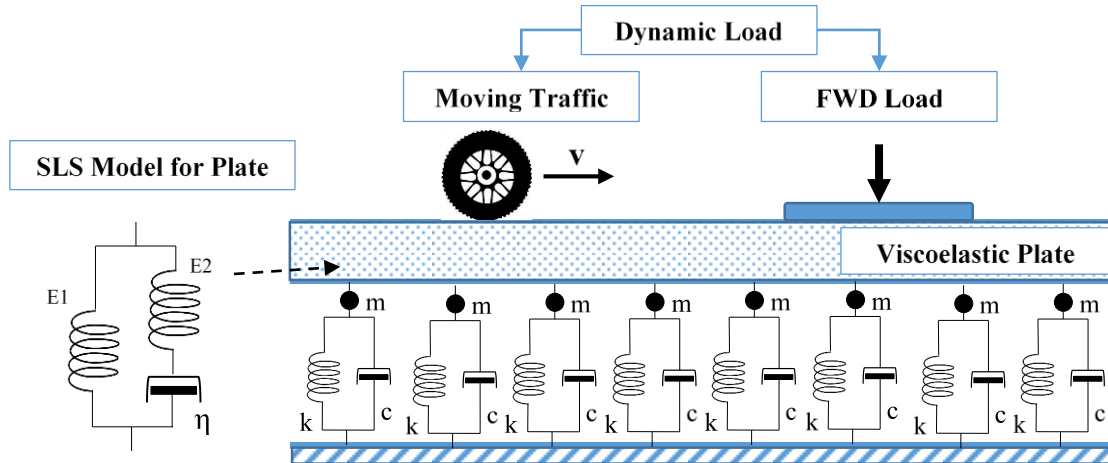
45

1           The purpose of this paper is to demonstrate how FWD measurements can be used by  
2 transportation agencies to evaluate deflection-induced vehicle fuel consumption. To this end, the  
3 PVI analysis is modified first to account for inertia and damping effects of the layers underlying  
4 the road surface. This modification makes the analysis compatible with the generalized  
5 Westergaard model. Next, one flexible and one rigid pavement section are selected from the  
6 database provided by the Long Term Pavement Performance (LTPP) program, each of which  
7 were tested multiple times at different months of a year. The model parameters were  
8 backcalculated for the selected pavement sections, and then employed as inputs to estimate the  
9 resulting fuel consumption. The variation in energy dissipation due to seasonal changes was also  
10 studied. The results confirm that the proposed methodology can be a reliable tool to evaluate  
11 deflection-induced vehicle fuel consumption and environmental footprint.

## 12 **THEORETICAL BACKGROUND**

13 The plate-on-a-foundation model has been commonly used for structural modeling of rigid  
14 pavements. Westergaard (17) idealized the rigid slab as a thin elastic Kirchhoff-Love plate  
15 resting on a Winkler foundation, which is a combination of closely spaced, independent elastic  
16 linear springs. Various researchers emphasized the more complex behavior of the foundation and  
17 added a dashpot to the Westergaard model to account for viscoelastic behavior of foundation  
18 (18-21). Also, the importance of foundation inertia effects was pointed out (22). Khazanovich  
19 demonstrated that the integrated inertia and damping effect can more accurately explain the  
20 behavior of pavement under dynamic loading, in particular, the time shift between the applied  
21 FWD load and the recorded deflection peaks (23). In a recent study, Khazanovich &  
22 Booshehrian proposed a generalized Westergaard model to account for viscoelasticity of the  
23 plate and the inertia and damping effects of foundation. They were able to show this model could  
24 accurately capture the pavement behavior under dynamic FWD loading for both flexible and  
25 rigid pavements (16).

26  
27           The generalized Westergaard model consists of an infinite viscoelastic plate resting on a  
28 foundation that takes into account inertia and damping effects of the foundation (FIGURE 1).  
29 The plate is modeled with a three-parameter standard linear solid (SLS) model to capture the  
30 viscoelastic behavior of flexible pavement. The damping and inertia effects of foundation are  
31 accounted for by the addition of dashpot and mass elements to the Winkler foundation. The mass  
32 element represents the mass of the plate and the moving portion of the underlying layers under  
33 applied dynamic loads. The combination of the spring and dashpot simulates the viscoelastic  
34 behavior of the underlying layers based on the Kelvin-Voigt model.  
35



1  
2  
3  
4  
5  
6  
7  
8  
9  
10  
11  
12  
13

**FIGURE 1 Generalized Westergaard Model**

In the following section, the generalized Westergaard model is incorporated into the PVI frameworks (11,15).

### Deflection-Induced PVI Model

Consider an infinite plate subjected to a moving load  $P = pS$  representing the wheel load, with  $S$  rectangular area of tire-road contact trajectory. Herein, we consider a moving coordinate system  $X = x - Vt$ , attached to the load traveling with constant speed  $V$ . For any viscoelastic material in this reference frame, one can show that the dissipated energy within the material is related to the slope in the moving direction at the road-tire contact trajectory (12). Assuming a uniformly distributed load, the dissipated energy per distance traveled,  $\delta U$ , reads:

$$\delta U = -P \left\langle \frac{dw}{dX} \right\rangle \quad (1)$$

14  
15  
16  
17  
18  
19  
20  
21  
22  
23  
24  
25  
26  
27  
28

where  $w$  is the plate deflection and  $\langle dw/dX \rangle$  is the average slope along the area of tire-road contact surface in  $X$ -direction. Hence, to evaluate the energy dissipation one needs to evaluate plate deflection and its spatial derivative in the moving coordinate system. Herein, we employ the elastic-viscoelastic correspondence principle (24-26) to evaluate deflection. The principle allows for finding the solution of a viscoelastic problem from the solution of a corresponding elastic problem in the frequency domain, by substituting the complex modulus of the viscoelastic material with its elastic counterpart.

Using the elastic-viscoelastic correspondence principle, first the solution to equation of motion of an elastic plate on an elastic foundation subjected to a moving load needs to be obtained in the frequency domain. Assuming a steady-state condition (constant speed), and noting that in the moving coordinate system  $\partial/\partial t = -V\partial/\partial X$ , the equation of motion in this reference frame reads:

$$D \left( \frac{\partial^2}{\partial X^2} + \frac{\partial^2}{\partial y^2} \right)^2 w + mV^2 \frac{\partial^2 w}{\partial X^2} + kw = p \quad (2)$$

1  
2 where  $D = Eh^3/12(1 - \nu^2)$  is plate's instantaneous flexural stiffness and  $m$  is mass per unit  
3 area of the plate and moving portion of foundation;  $E$ ,  $h$ , and  $\nu$  are instantaneous modulus of  
4 elasticity, thickness, and Poisson's ratio of the surface layer (plate), respectively. Taking the  
5 Fourier transformation of the above solution in frequency domain gives:  
6

$$\hat{w} = \hat{p} (D(\lambda_1^2 + \lambda_2^2)^2 - mV^2\lambda_1^2 + k)^{-1} \quad (3)$$

7  
8 where  $\lambda_1$  and  $\lambda_2$  are respectively the transformed fields of  $X$  and  $y$ .  
9

10 To find the solution of a viscoelastic plate on a viscoelastic foundation, the following  
11 approach was taken. The stress-strain relationship of the viscoelastic top layer is according to the  
12 constitutive equation of a standard linear solid (SLS) model (illustrated in the inset of FIGURE  
13 1).  
14

$$\frac{\partial \varepsilon}{\partial t} = \frac{1}{E_1 + E_2} \left( \frac{\partial \sigma}{\partial t} + \frac{1}{\eta} (E_2 \sigma - E_1 E_2 \varepsilon) \right) \quad (4)$$

15  
16 where  $E_1$ ,  $E_2$  are two stiffness parameters of the model. In addition,  $\eta$  is the material viscosity  
17 parameter, and therefore,  $\tau = \eta/E_2$  is the relaxation time of the viscoelastic top-layer. Damping  
18 of foundation is modeled via a Kelvin-Voigt viscoelastic foundation with stiffness  $k$  and  
19 relaxation time  $\tau_s = c/k$ , where  $c$  is viscous damping coefficient of foundation as illustrated in  
20 FIGURE 1. To incorporate the viscoelasticity of foundation, the elastic foundation modulus  $k$  is  
21 replaced with the complex modulus of a Kelvin-Voigt model in the moving coordinate system,  
22 i.e.  $\hat{k} = k(1 - i\lambda_1 V \tau_s)$ .

23 For the SLS model representing the material of surface layer (plate), we first rewrite  
24 equation (4) in the moving coordinate system:  
25

$$-V \frac{d\varepsilon}{dX} = \frac{1}{E_1 + E_2} \left( -V \frac{d\sigma}{dX} + \frac{1}{\eta} (E_2 \sigma - E_1 E_2 \varepsilon) \right) \quad (5)$$

26  
27 Here we assume a three-dimensional creep behavior characterized by constant creep Poisson's  
28 ratio such that  $\hat{D} = \hat{E}h^3/12(1 - \nu^2)$ . Then, taking Fourier transform of equation (5), the  
29 complex modulus can be obtained  $\hat{D} = D_1(1 - i\lambda_1 V \tau (D_2/D_1 + 1))/(1 - i\lambda_1 V \tau)$  where  $D_1 =$   
30  $E_1 h^3/12(1 - \nu^2)$  and  $D_2 = E_2 h^3/12(1 - \nu^2)$ . The solution for the viscoelastic problem in the  
31 frequency domain is expressed as:  
32

$$\hat{w} = \hat{p} \left( \frac{1 - i\lambda_1 V \tau (D_2/D_1 + 1)}{1 - i\lambda_1 V \tau} D_1 (\lambda_1^2 + \lambda_2^2)^2 - mV^2 \lambda_1^2 + k(1 - i\lambda_1 \tau_s) \right)^{-1} \quad (6)$$

33  
34 The viscoelastic plate deformation is obtained by taking the inverse Fourier  
35 transformation of above equation. The slope  $dw/dX$  is also similarly calculated from  
36  $\mathcal{F}^{-1}(-i\lambda V \hat{w})$  with  $\mathcal{F}^{-1}$  denoting the inverse Fourier transformation.

1 The procedure above offers a computationally efficient approach for determining  
 2 pavement deflections and energy dissipation under a moving load using the generalized  
 3 Westergaard model. However, to ensure that the estimation of the energy dissipation is realistic,  
 4 it is important to select appropriate values for model parameters that will result in calculated  
 5 deflections similar to those exhibited by the pavement system. These quantities can be obtained  
 6 from the dynamic backcalculation analysis of FWD data as explained below.

### 8 **Dynamic Backcalculation of Pavement Parameters Using FWD Data**

9  
 10 FWD measures the time histories of the applied load and surface deflections at different  
 11 distances from the center of a circular FWD applied pressure. Thus the governing differential  
 12 equation for an infinite, homogeneous, isotropic, and linearly viscoelastic plate on a viscoelastic  
 13 foundation subjected to axisymmetric FWD loading is:

$$14 \quad D' \left( \frac{1}{r} \frac{\partial}{\partial r} + \frac{\partial^2}{\partial r^2} \right)^2 w(r, t) + k w(r, t) + c \frac{\partial w(r, t)}{\partial t} + m \frac{\partial^2 w(r, t)}{\partial t^2} = p(r, t) \quad (7)$$

15  
 16 where  $D'$  is the viscoelastic rigidity of the plate that can be calculated based on stress-strain  
 17 relationship of the viscoelastic top layer given in equation (4),  $w(r, t)$  is the surface  
 18 deflection,  $p(r, t)$  is the applied pressure in the FWD test,  $r$  is the distance from the center of  
 19 FWD load, and  $t$  is the time. The pressure,  $p(r, t)$ , is obtained from measurements in the FWD  
 20 tests, and is not necessarily a mathematical function, therefore equation (7) must be solved  
 21 numerically. Khazanovich & Booshehrian (16) proposed a numerical solution for this equation  
 22 using a combined application of Hankel transform in space and finite difference method in time.  
 23 Taking advantage of the time domain approach prevents the potential problems of using  
 24 frequency domain such as the need for tail correction (27-29).

25  
 26 The obtained semi-analytical solution is used as a forward solution in the backcalculation  
 27 procedure. A normalized sum of squared errors (SSE) is defined to quantify the difference  
 28 between the measured and calculated FWD deflections. A combination of quasi-Newton method  
 29 and a finite-difference gradient is employed to find the solution to the inverse problem, which is  
 30 to find the set of parameters that minimizes the following error function.

$$31 \quad SSE = \left( \frac{1}{w_{max}^M} \right)^2 \sum_{i=1}^n \sum_{j=1}^m (w_{ij}^M - w_{ij}^C)^2 \quad (8)$$

32  
 33 where  $n$  is the number of sensors,  $m$  is the number of time steps in the FWD deflection time  
 34 history,  $w_{ij}^M$  and  $w_{ij}^C$  are the measured and calculated deflections for sensor  $i$  at time  $j$ ,  
 35 respectively, while  $w_{max}^M$  is the maximum measured deflection in the FWD deflection history.  
 36 The error is normalized by dividing by  $w_{max}^M$ , so that their non-dimensional SSE values can be  
 37 compared. The parameters to be determined from the backcalculation procedure are 1) the plate's  
 38 instantaneous flexural stiffness,  $E$ , 2) the ratio  $E_l/E$ , and 3) the relaxation time of the plate  
 39 material,  $\tau$ , 4) foundation stiffness,  $k$ , 5) foundation inertia,  $m$ , and 6) damping coefficient of the  
 40 foundation,  $c$ .

## 1 CASE STUDY

2 The previous section describes how the pavement-vehicle interaction (PVI) model was modified  
 3 according to the generalized Westergaard model to account for inertia and damping effects of  
 4 underlying layers. This section illustrates how the model parameters, backcalculated using the  
 5 FWD data, can be used in the implementation of the PVI model to estimate the vehicle fuel  
 6 consumption due to pavement deformation for both rigid and flexible pavements. This section  
 7 also examines if the developed procedure is able to address the seasonal variations in pavement  
 8 system and provide acceptable estimations of fuel consumption. Especially when considering  
 9 flexible pavements fabricated with a hot mix asphalt (HMA) course as the surface layer,  
 10 temperature variation could considerably influence the viscoelastic properties of the asphaltic  
 11 material, and thus, the amount of energy dissipated through PVI.

12  
 13 The FWD data collected through the “Seasonal Monitoring Program (SMP)” of the Long  
 14 Term Pavement Performance (LTPP) program were used in this study (30). The SMP study did  
 15 not contain a set of flexible and rigid pavements located in fairly similar locations, so pavements  
 16 with relatively similar sublayers were chosen: a flexible pavement located in Nevada (ID =  
 17 320101) and a rigid pavement located in North Carolina (ID = 370201). Both sections were in  
 18 good condition in year 2000. Details of the pavement sections are described in Table 1.

19  
 20 **TABLE 1 Detailed Information on the Selected Pavement Sections**

Location / Section ID	Pavement Type	Surface Layer	Thickness (m) / Density (kg/m <sup>3</sup> )	Base layer / Thickness (m)	Subbase layer / Thickness (m)	Subgrade Type
NV / NV0101	Flexible	HMA	0.1829 / 2234	Agg. / 0.208	Agg./ 0.579 + Treated/ 0.305	Coarse Grained
NC / NC0201	Rigid	PCC	0.2337/ 2240	Agg. / 0.236	Treated/ 0.203	Fine Grained

21  
 22 A Poisson’s ratio of 0.15 was assumed for the rigid pavement and 0.35 for the flexible  
 23 pavement. FWD tests were performed at the center of the slab, away from the pavement edge  
 24 (J1 loading). The same location of the pavement section was investigated at different times of the  
 25 year. Further information on the two sections studied here can be found on InfoPave™, the  
 26 online LTPP database (30).

## 27 RESULTS

28 Six FWD deflection measurements for the flexible section (NV0101) and five FWD deflection  
 29 measurements for the rigid section (NC0201) collected in year 2000 were used for this study.  
 30 The sections were analyzed using the dynamic backcalculation procedure described in the  
 31 previous section (16) and the results are summarized in Table 2 along with the month and surface  
 32 temperature of the FWD testing. The backcalculated parameters were then used to calculate the  
 33 deflection basins. The time history of measured and calculated surface deflections at different  
 34 sensor locations (0.0 to 1.5 m) are shown in Figures 2 (sections NV0101) and 3 (section  
 35 NC0201).

36  
 37 The backcalculated model parameters were ultimately used in the modified PVI model to  
 38 compute the dissipated energy and fuel consumption under a moving vehicle load. The analysis  
 39 was performed at typical highway speed of 100 Km/hr for an HS-20 (a 20 ton semi-trailer truck).  
 40 The tire-road contact surface was assumed to be a square with dimension of 0.15 x 0.15 m. The

1 dissipated energy per distance traveled was calculated based on equation (1). The associated fuel  
 2 consumption is obtained by dividing the dissipated energy by the energy content of fuel which is  
 3 equal to 38.74 MJ/liter for Diesel (*I*). The results of this analysis are summarized in Table 3  
 4 together with the month and surface temperature at the time of FWD tests.  
 5  
 6

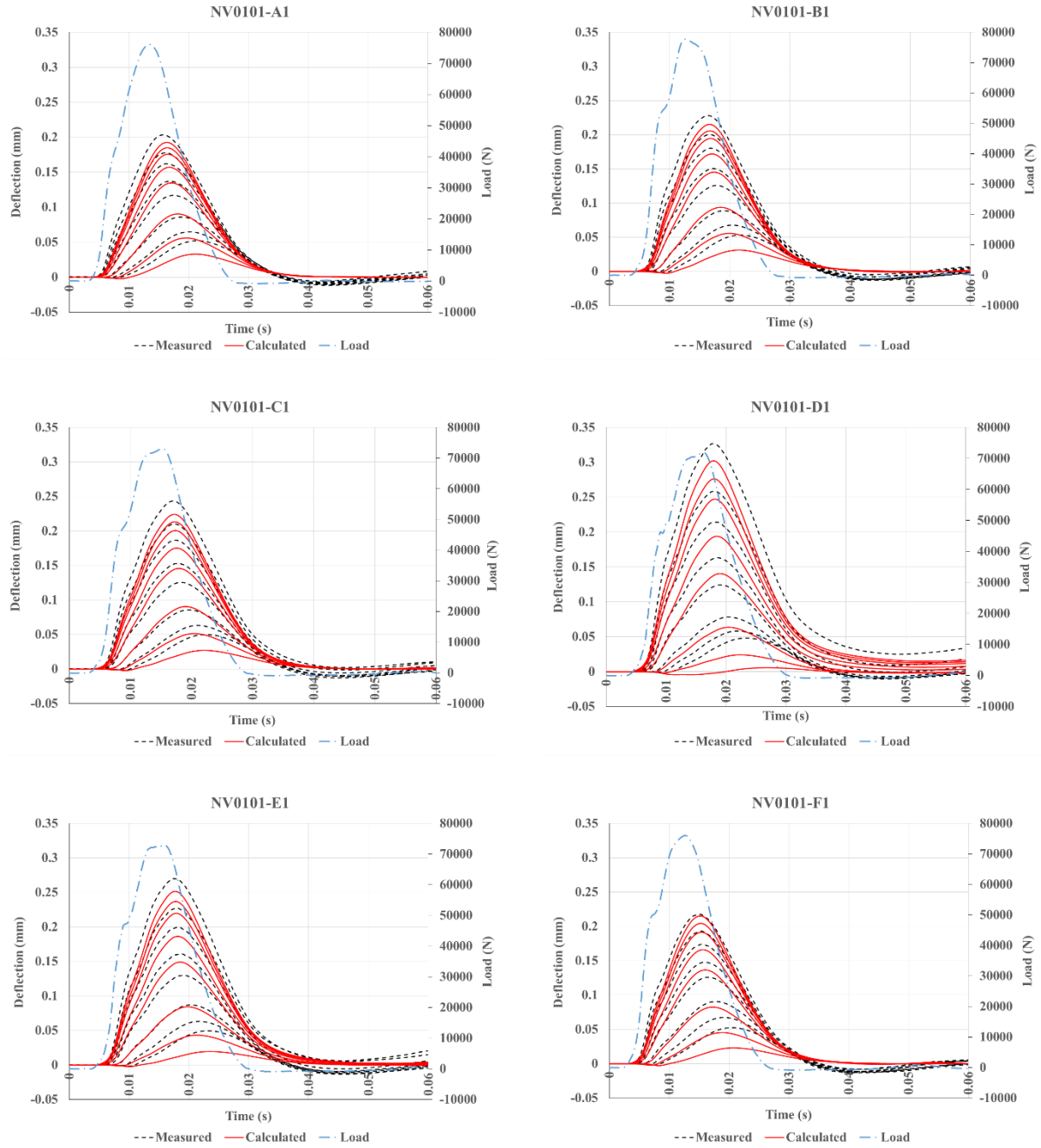
**TABLE 2 Backcalculated Pavement Parameters Based on the FWD Deflection Basins**

Pavement Type	ID	Month	Surface Temp.	Foundation Parameters			Plate Parameters			Error
			°C	k	m	c	E	E1/E	τ	
				KPa/mm	kg/m <sup>2</sup>	Ns/m/m <sup>2</sup>	GPa	-	s	
Flexible (NV0101)	A1	Feb	1.4	92.83	1102.2	7.07E+05	26.53	1.00	-	6.98
	B1	Mar	16.5	92.93	822.2	7.08E+05	22.05	1.00	-	7.04
	C1	May	18.2	96.50	662.0	6.87E+05	18.95	0.93	4.95	6.71
	D1	Aug	34.9	143.59	408.8	7.77E+05	8.63	0.51	2.28	9.41
	E1	Sep	23.7	102.87	408.8	7.31E+05	13.90	0.81	6.31	7.50
	F1	Nov	3.9	91.24	998.3	6.64E+05	23.80	1.00	-	7.25
Rigid (NC0201)	B1	Feb	11.2	32.46	838.2	3.47E+05	34.73	1.00	-	1.88
	C1	Mar	13.8	34.25	1158.7	3.98E+05	34.93	1.00	-	2.44
	E1	May	26.5	30.09	1529.9	3.59E+05	33.80	1.00	-	6.81
	F1	Aug	36.2	30.16	1308.0	3.52E+05	33.17	1.00	-	3.07
	G1	Sep	32.7	32.46	963.9	3.75E+05	33.83	1.00	-	2.73

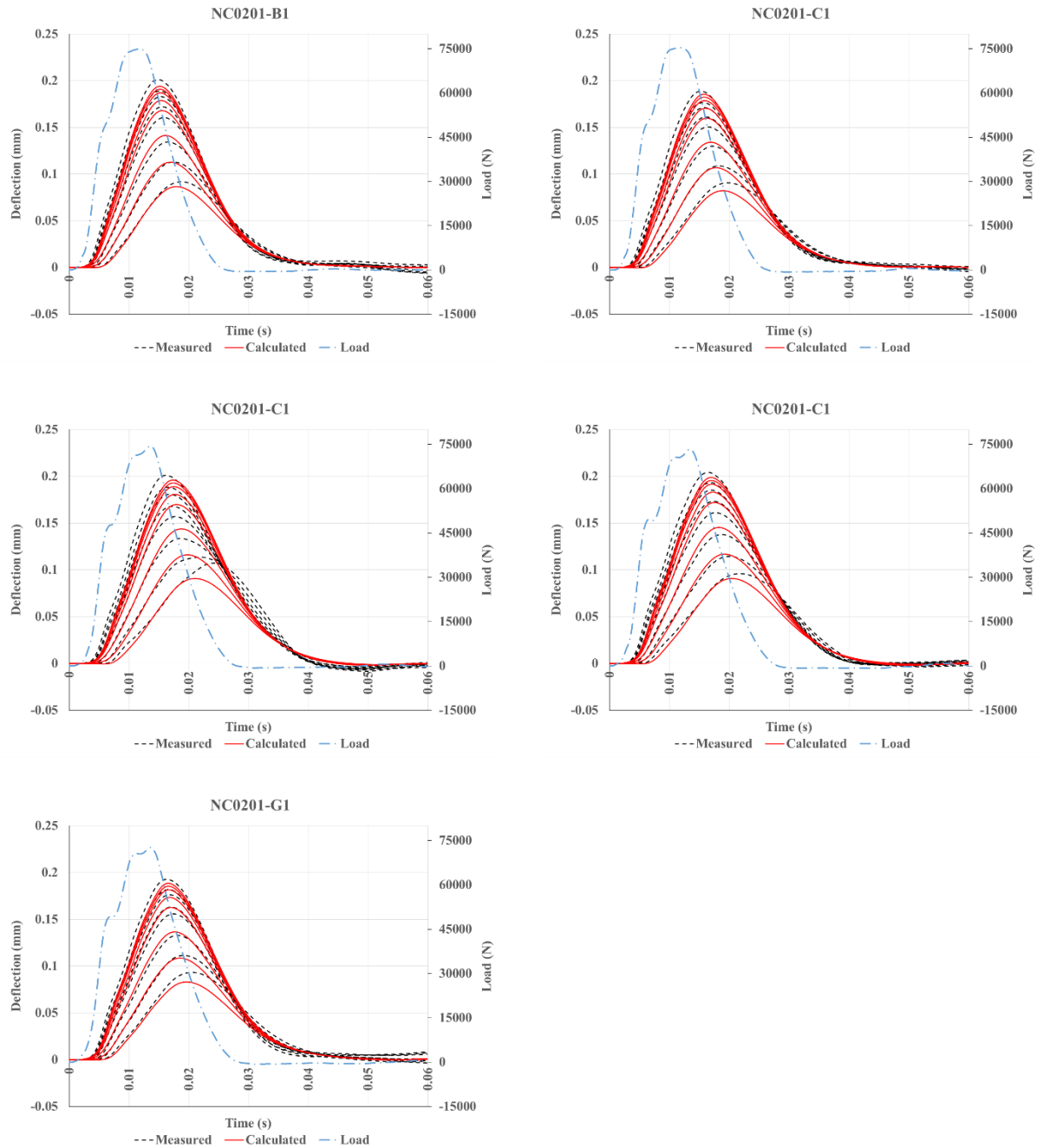
**TABLE 3 Results of Energy Dissipation Analyses Using the Backcalculated Pavement Parameters**

Pavement Type	ID	Month	Surface Temp.	Dissipation Rate	Dissipation	Fuel Consumption
			°C	(J/Sec)	(MJ/Km)	(Gal/mile)
Flexible (NV0101)	A1	Feb	1.4	163.22	5.88E-03	6.45E-05
	B1	Mar	16.5	195.82	7.05E-03	7.74E-05
	C1	May	18.2	212.14	7.64E-03	8.38E-05
	D1	Aug	34.9	362.40	1.30E-02	1.43E-04
	E1	Sep	23.7	293.28	1.06E-02	1.16E-04
	F1	Nov	3.9	173.23	6.24E-03	6.84E-05
Rigid (NC0201)	B1	Feb	11.2	87.61	3.15E-03	3.46E-05
	C1	Mar	13.8	108.11	3.89E-03	4.27E-05
	E1	May	26.5	103.80	3.74E-03	4.10E-05
	F1	Aug	36.2	101.94	3.67E-03	4.03E-05
	G1	Sep	32.7	104.60	3.77E-03	4.13E-05

10  
11



1 **FIGURE 2 Measured and Calculated FWD Deflection Basins for Flexible Pavement**  
2 **(NV0101) in Nevada at Different Months**  
3



1 **FIGURE 3 Measured and Calculated FWD Deflection Basins for Rigid Pavement**  
 2 **(NC0201) in North Carolina at Different Months**

3 **DISCUSSION**

4 The backcalculated pavement parameters are reliable if the measured and calculated FWD  
 5 deflection basins are in close agreement with each other, confirming that the backcalculated  
 6 parameters are capable of appropriately describing the pavement behavior under dynamic  
 7 loading. The agreement of the measured and calculated results illustrated in Figures 2 and 3  
 8 indicates that the proposed method is an effective tool for evaluating the properties of pavement  
 9 sections.

1  
2 The results of the analyses on the SMP sections (NV0101 and NC0201), shown in Table  
3 2, reveals that the properties of the PCC layer in the selected rigid pavement remained almost  
4 constant and the PCC plate behaved elastically regardless of the seasonal/temperature variations.  
5 The foundation properties, except for foundation viscosity exhibited relatively higher variability,  
6 in particular the foundation inertia effect. On the other hand, for flexible pavement, the  
7 temperature variation and seasonal changes caused considerable changes in the properties of both  
8 the plate (HMA course) and the foundation (underlying layers). Both coefficients of subgrade  
9 reaction and foundation inertia effect varied significantly with the temperature change while the  
10 foundation viscosity did not encounter significant changes. The instantaneous elastic modulus of  
11 the HMA plate altered proportionally with the surface temperature change. The plate behaved  
12 elastically at the colder periods of the year (Feb, Mar, and Nov) and became more viscous as the  
13 temperature increased. The obtained backcalculated parameters were in line with the  
14 expectations of the behavior of rigid and flexible pavements.

15  
16 Figure 4 depicts the variation of fuel consumption and testing temperature throughout the  
17 year 2000. Figure 4 clearly demonstrates the dependency of the vehicle energy consumption on  
18 the temperature change for flexible pavements. An increase in the temperature made the HMA  
19 surface more viscous, resulting in more viscoelastic deformation and a higher amount of  
20 deflection-induced dissipation of energy. In contrast, based on the backcalculated plate  
21 parameters, shown in Table 2, the PCC layer behaved elastically regardless of the seasonal  
22 variation, and the dissipation due to the plate deformation is insignificant. Interestingly, the  
23 consumed fuel for rigid pavements plotted in Figure 4 was a consequence of viscoelastic  
24 properties of the underlying layer and not the surface layer. The backcalculated damping  
25 coefficient of foundation showed minor variation in the pavement section in North Carolina (see  
26 Table 2), which made the vehicle fuel consumption independent from temperature variation for  
27 the selected rigid pavement in this region. It is important to note that the fuel consumption  
28 caused by foundation viscoelasticity might vary considerably in regions that encounter  
29 considerable seasonal variation in the soil properties.

30  
31 Overall, based on the observations made in this study, the proposed method — dynamic  
32 backcalculation analyses using FWD time history data followed by the modified deflection-  
33 induced PVI analyses — provided reasonable results, which are in agreement with realistic  
34 expectations and field observations. Since FWD testing is a common pavement evaluation  
35 practice, the proposed method could be used widely to perform network scale analyses. The  
36 estimated deflection-induced energy dissipation and vehicle fuel consumption could potentially  
37 be incorporated as a factor in pavement management and in future network planning to reduce  
38 greenhouse gas (GHG) emissions and design more sustainable roads (15). It is necessary to note  
39 that the proposed approach still has to be tested and validated via field measurements of fuel  
40 consumption for various site conditions and pavement structures.

41  
42 The proposed tool shows reasonable results for the sections analyzed in this study, yet the  
43 model can still benefit from improvement. A few possible improvements are discussed here.

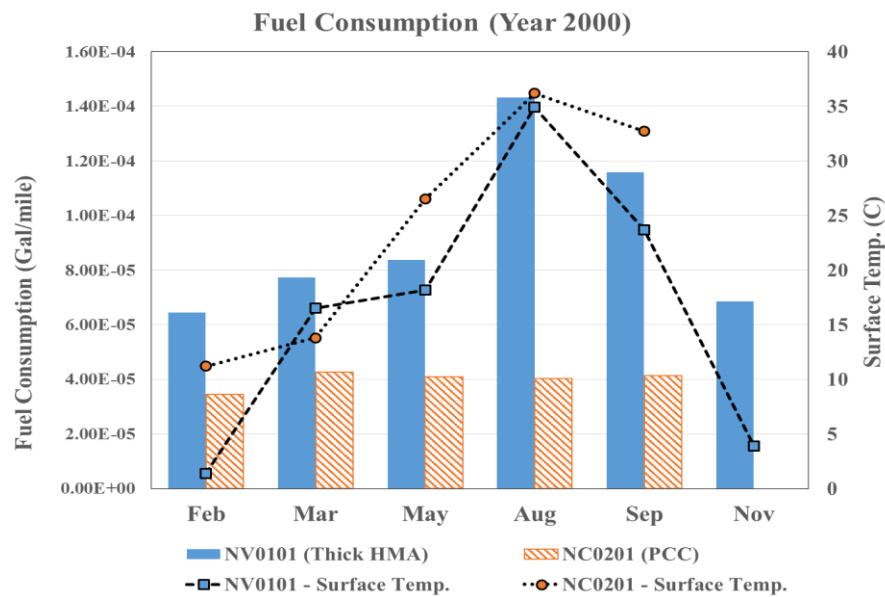
44 The results in Figures 2 and 3 show that the discrepancy between the curves is smaller for  
45 the rigid section than for a relatively thick flexible pavement. One reason might be that the  
46 generalized Westergaard model employed in this study ignores the shear resistance of the

1 underlying layers. While this assumption may be realistic for rigid pavements, it may not hold  
 2 true for flexible pavements, especially when the top layer is thin. Thus, one important adjustment  
 3 to the model could be including shear resistance in the foundation model, especially for flexible  
 4 pavements. Making use of the Pasternak model could be a solution to this issue.  
 5

6 In addition, the viscoelastic Kirchhoff-Love plate adopted in this study does not account  
 7 for shear deformation and compressibility of the surface layer, which might be important  
 8 properties for HMA layers. However, these properties are more influential in flexible pavements  
 9 constructed with thicker HMA layers as seen in full-depth asphalt pavements. Those pavements  
 10 were not the topic of this study.  
 11

12 Another important factor to improve is accounting for the effect of daily temperature  
 13 change on the properties of the flexible pavement and on fuel consumption. This effect could  
 14 have considerable impact on estimating the use-phase GHG emissions. One solution for  
 15 addressing this issue is to perform similar analyses on multiple sets of FWD tests conducted on  
 16 the same day to capture the effect of daily temperature variation on the properties of pavement  
 17 system, and to define/introduce correction factors.  
 18

19 It is worth noting that the PVI analysis herein assumes an infinite plate and does not  
 20 consider the impact of joints spacing and characteristics on vehicle fuel consumption. Neglecting  
 21 the joints impact might underestimate the deflection-induced energy dissipation for rigid  
 22 pavements. However, this impact is local and can only be considerable at locations very close to  
 23 the joints. Further investigation is required to quantify the variation in fuel consumptions close to  
 24 the joints.  
 25



26 **FIGURE 4 Effect of Seasonal Variation on the Dissipation Rate for both Flexible and Rigid**  
 27 **Pavements**  
 28

## 1 CONCLUSIONS

2 In this study, the structural parameters of the tested pavement sections are backcalculated by  
3 minimizing the difference between the time histories of deflections measured via FWD and the  
4 deflections calculated using the generalized Westergaard model. The backcalculated parameters  
5 are then used to estimate the vehicle fuel consumption due to deflection-induced pavement-  
6 vehicle interaction. The described procedure allows for establishing a link between the structural  
7 parameters of rigid and flexible pavements, and vehicle fuel consumption and greenhouse gas  
8 (GHG) emissions during the pavement use-phase. **The purpose of this study is to show that the**  
9 **proposed method can be used to estimate the fuel consumption related to both asphalt and**  
10 **concrete pavements. Since the two tested pavement sections were not structurally equivalent,**  
11 **direct comparison is not possible.** The following general conclusions can be drawn from this  
12 study:

- 14 - Modifying the PVI model to be compatible with the generalized Westergaard model  
15 allows it to take into account the impact of foundation damping and inertia.
- 16 - It is shown that the generalized Westergaard model is able to capture the behavior of both  
17 rigid and flexible pavements under dynamic loading with good accuracy, which makes  
18 the assignment of model parameter for PVI analysis more reliable.
- 19 - The proposed methodology is able to describe the pavement structural changes due to  
20 seasonal variation for the selected rigid and flexible pavement sections. The energy is  
21 dissipated through the viscous deformation of both the surface layer and underlying  
22 layers.
- 23 - Seasonal variations affect the amount of fuel consumption throughout a year for flexible  
24 pavement mainly due to the noticeable variation in the temperature and the corresponding  
25 change in viscoelastic properties of the HMA surface course.
- 26 - A significant portion of energy dissipation occurs in the foundation. Thus, ignoring this  
27 effect may lead to underestimation of the energy dissipation, especially for rigid  
28 pavements.
- 29 - The simplicity of the described model and the availability of FWD measurements makes  
30 the proposed methodology an attractive tool for performing network scale analyses and,  
31 potentially, for designing more sustainable roads.

33 Good fit was obtained in the performed analyses for the two tested pavement sections;  
34 however, there is still a room for improvement of the generalized Westergaard model, in  
35 particular for flexible pavements. **One possible modification is to use a foundation model that**  
36 **incorporates the shear contribution of the foundation.** The applicability of this model for a wider  
37 range of pavement systems and climatic conditions, such as a thin HMA layer, should be further  
38 investigated. The effect of daily temperature change on the viscoelastic properties of the HMA  
39 layer and energy dissipation must be evaluated in future studies. **Further studies should**  
40 **investigate the contribution of joints spacing and joints characteristics to the energy dissipation.**

## 41 ACKNOWLEDGMENT

42 This research was carried out by the CSHub@MIT with sponsorship provided by the Portland  
43 Cement Association (PCA), the Ready Mixed Concrete (RMC) Research & Education  
44 Foundation, and the Minnesota Department of Transportation (MnDOT). The authors are solely  
45 responsible for the content.

**REFERENCES**

1. Ardekani, S. A., and P. Sumitsawan. Effect of pavement type on fuel consumption and emissions in city driving, <http://www.rmc-foundation...20Study%20Final%203-10.pdf>, 2010
2. Gschsser, F., and H. Wallbaum. Life Cycle Assessment of Representative Swiss Road Pavements for National Roads with an Accompanying Life Cycle Cost Analysis. *Environmental Science & Technology*, Vol. 47, 2013, pp. 8453-8461.
3. Chatti, K., and I. Zaaber. Estimating the effects of pavement condition on vehicle operating costs. *NCHRP Report 720*. Transportation Research Board of the National Academies, Washington, D.C., 2012.
4. Louhghalam, A., Tootkaboni, M., and F. J. Ulm. Roughness-Induced Vehicle Energy Dissipation: Statistical Analysis and Scaling. *Journal of Engineering Mechanics*, 2015, 04015046.
5. Louhghalam, A., Akbarian, M., and F. J. Ulm, Roughness-induced pavement-vehicle interactions: Key parameters and impact on vehicle fuel consumption. *Accepted for publication in Transportation Research Record: Journal of the Transportation Research Board*, 2015.
6. Zaabar, I., and K. Chatti. Calibration of HDM-4 models for estimating the effect of pavement roughness on fuel consumption for US conditions. In *Transportation Research Record: Journal of the Transportation Research Board*, No. 2155, Transportation Research Board of the National Academies, Washington, D.C., 2010, pp. 105-116.
7. Zaabar, I., and K. Chatti. New mechanistic-empirical approach for estimating the effect of roughness on vehicle durability. In *Transportation Research Record: Journal of the Transportation Research Board*, No. 2227, Transportation Research Board of the National Academies, Washington, D.C., 2011, pp. 180-188.
8. Wang, T., Harvey, J., and A. Kendall. Reducing greenhouse gas emissions through strategic management of highway pavement roughness. *Environmental Research Letters*, Vol. 9, No. 3, 2014, 034007.
9. Pouget, S., Sauzéat, S., Benedetto, H.D., and F. Olard. Viscous energy dissipation in asphalt pavement structures and implication for vehicle fuel consumption. *Journal of Materials in Civil Engineering*, Vol. 24, No. 5, 2011, pp. 568-576.
10. Chupin, O., Piau, J. M., and A. Chabot. Evaluation of the structure-induced rolling resistance (SRR) for pavements including viscoelastic material layers. *Journal of Materials and structures*, Vol. 46, No. 4, 2013, pp. 683-696.
11. Pouget, S., Sauzéat, S., Benedetto, H.D., and F. Olard. Calculation of viscous energy dissipation in asphalt pavements. *Baltic Journal of Road and Bridge Engineering*, Vol. 9, No. 2, 2014, pp. 123-130.
12. Louhghalam, A., Akbarian, M., and F. J. Ulm. Flügge's Conjecture: Dissipation-versus Deflection-Induced Pavement-Vehicle Interactions. *Journal of Engineering Mechanics*, Vol. 140, No. 8, (04014053), 2013.
13. Louhghalam, A., Akbarian, M., and F. J. Ulm. Scaling relations of dissipation-induced pavement-vehicle interactions. *Transportation Research Record, Journal of the Transportation Research Board*, No. 2457, Transportation Research Board of the National Academies, Washington, D.C., 2014, pp. 95-104.

- 1 14. Louhghalam, A., Akbarian, M., and F. J. Ulm. Pavement Infrastructures Footprint: The  
2 Impact of Pavement Properties on Vehicle Fuel Consumption, *Proceedings of Computational*  
3 *Modelling of Concrete Structures*. EURO-C, 2014.
- 4 15. Louhghalam, A., Akbarian, M., and F. J. Ulm. Carbon Management of Infrastructure  
5 Performance: Integrated Big Data Analytics and Pavement-Vehicle-Interactions, *under*  
6 *review*, 2015.
- 7 16. Khazanovich, L., and A. Booshehrian. Dynamic visco-elastic analysis of falling weight  
8 deflectometer deflections for rigid and flexible pavements. *Accepted for publication in*  
9 *Transportation Research Record: Journal of the Transportation Research Board*, 2015.
- 10 17. Westergaard, H. M. Stresses in concrete pavements computed by theoretical analysis. *Public*  
11 *Roads*, Vol. 7, No. 2, 1926, pp. 25-35.
- 12 18. Kim, Y., and Y. R. Kim. Prediction of layer moduli from falling weight deflectometer and  
13 surface wave measurements using artificial neural network. In *Transportation Research*  
14 *Record: Journal of the Transportation Research Board*, No. 1639, Transportation Research  
15 Board of the National Academies, Washington, D.C., 1998, pp. 53-61.
- 16 19. Kutay, M. E., Chatti, K., and L. Lei. Backcalculation of Dynamic Modulus Mastercurve from  
17 Falling Weight Deflectometer Surface Deflections. In *Transportation Research Record:*  
18 *Journal of the Transportation Research Board*, No. 2227, Transportation Research Board of  
19 the National Academies, Washington, D.C., 2011, pp. 87-96.
- 20 20. Kuo, C. M., and T. Y. Tsai. Significance of subgrade damping on structural evaluation of  
21 pavements. *Road Materials and Pavement Design*, Vol. 15, No. 2, 2014, pp. 455-464.
- 22 21. Kuo, C. M., Lin, C. C., Huang, C. H., and Y. C. Lai. Issues in simulating falling weight  
23 deflectometer test on concrete pavements. *KSCE Journal of Civil Engineering*, 2015, pp. 1-7.
- 24 22. Sebaaly, B. E., Mamlouk, M. S., and T. G. Davies. Dynamic analysis of falling weight  
25 deflectometer data. In *Transportation Research Record: Journal of the Transportation*  
26 *Research Board*, No. 1070, Transportation Research Board of the National Academies,  
27 Washington, D.C., 1986, pp. 63-68.
- 28 23. Khazanovich, L. Dynamic analysis of FWD test results for rigid pavements. *Symposium on*  
29 *Nondestructive Testing of Pavements and Backcalculation of Moduli*, ASTM STP 1375,  
30 American Society for Testing and Materials, West Conshohocken, PA, Vol. 3, 2000, pp. 398-  
31 411.
- 32 24. Pozhuev, V. Steady-state reaction to the effect of a moving load in a system consisting of a  
33 cylindrical shell and a viscoelastic filler, *International Journal of Applied Mechanics*. Vol.  
34 22, No. 5, 1986, pp. 415-421.
- 35 25. Read, W. T. Stress analysis for compressible viscoelastic materials. *Journal of Applied*  
36 *Physics*, Vol. 21, No. 7, 1950, pp. 671-674.
- 37 26. Christensen, R. Theory of viscoelasticity: An introduction, *Academic Press*, New York,  
38 1982.
- 39 27. Uzan, J. Dynamic linear back calculation of pavement material parameters. *Journal of*  
40 *transportation engineering*, Vol. 120, No. 1, 1994, pp. 109-126.
- 41 28. Chatti, K. Use of Dynamic Analysis for Interpreting Pavement Response. *Materials*  
42 *Evaluation*, Vol. 62, No. 7, 2004, pp. 764-774.
- 43 29. Zaabar, I., Chatti, K., Lee, H. S., and N. Lajnef. Backcalculation of asphalt concrete modulus  
44 master curve from field measured falling weight deflectometer data using a new time domain

- 1 viscoelastic dynamic solution and genetic algorithm. In *Transportation Research Record:*
- 2 *Journal of the Transportation Research Board*, No. 2475, Transportation Research Board of
- 3 the National Academies, Washington, D.C., 2014, pp. 80-92.
- 4 30. FHWA, U.S. Department of Transportation. LTPP: Long-Term Pavement Performance
- 5 Program. <http://www.infopave.com/> Accessed 2015.